

# Ballistics Image Processing and Analysis for Firearm Identification

Dongguang Li

*School of Computer and Security Science  
Faculty of Computing, Health and Science  
Edith Cowan University  
2 Bradford Street, Mount Lawley,  
Western Australia 6050*

## 1. Introduction

The identification of firearms from forensic ballistics specimens is an exacting and intensive activity performed by specialists with extensive experience. The introduction of imaging technology to assist the identification process of firearms has enhanced the ability of forensic ballisticians to conduct analyses of these specimens for identification.

The positive identification of ballistics specimens from imaging systems are important applications of technology in criminal investigation [1] [2] [3] [4]. While the image capture methodology for persons and forensic ballistics specimens is similar, the process of identification for each is dependent upon the level of certainty required for the identification.

The forensic identification of ballistics specimens relies on the detection, recognition and ultimate matching of markings on the surfaces of cartridges and projectiles made by the firearms [5]. Traditional methods for the comparison of these marks are based on incident light microscopy. The image formed from the oblique illumination of the mark gives a representation of the surface of the specimen in the region of the mark [6]. This representation is critically dependent on the material of the surface on which the marks have been made, and the geometry and intensity of the illumination system. The assessment by the ballisticians of the similarity between comparable marks on respective ballistics specimens from crime scenes and test firings will be based on the expertise and experience of the technologist. Thus the traditional method of matching markings has inherent difficulties, and entails an element of subjectivity [7].

The need for firearm identification systems by police services continues to increase with greater accessibility to weapons in the international contexts. The characteristic markings on the cartridge and projectile of a bullet fired from a gun can be recognized as a *fingerprint* for identification of the firearm [8]. Forensic ballistics imaging has the capacity to produce high-resolution digital images of cartridge cases and projectiles for matching to a library of ballistics images [9]. However, the reliance upon imaging technologies makes identification of ballistics specimens both a demanding and exacting task, where the control of the error of

Source: Image Processing, Book edited by: Yung-Sheng Chen,  
ISBN 978-953-307-026-1, pp. 572, December 2009, INTECH, Croatia, downloaded from SCIYO.COM

measurement in the imaging technique must not allow compromise of integrity of the identification process.

The analysis of marks on bullet casings and projectiles provides a precise tool for identifying the firearm from which a bullet is discharged [1] [10]. The characteristic markings of each cartridge case and projectile are released ready for analysis when the gun is fired. More than thirty different features within these marks can be distinguished, which in combination produce a “fingerprint” for identification of the firearm [11]. This forensic technique has wide application in the world of forensic science, and would play a vital part in legal evidence in the case where firearms are involved.

Projectile bullets fired through the barrel of a gun will exhibit extremely fine striation markings, some of which are derived from minute irregularities in the barrel, produced during the manufacturing process. The examination of these striations on land marks and groove marks of the projectile is difficult using conventional optical microscopy. However, digital imaging techniques have the potential to detect and identify the presence of striations on ballistics specimens.

Given a means of automatically analyzing features within such a firearm “fingerprint”, identifying not only the type and model of a firearm, but also each individual weapon as effectively as human fingerprint identification can be achieved. Due to the high demand of skill and the intensive nature of ballistics identification, law enforcement agencies around the world have expressed considerable interest in the application of ballistics imaging identification systems to both greatly reduce the time for identification and to introduce reliability (or repeatability) to the process.

Several ballistics identification systems are already available either in a commercial form or in a beta-testing state. The two major international ballistics imaging systems are manufactured by the IBIS Company in Montreal, Canada and the FBI (Drugfire) in USA. A Canadian company, Walsh Automation, has developed a commercial system called “Bulletproof”, which can acquire and store images of projectiles and cartridge cases, and automatically search the image database for particular striations on projectiles. However the user must match the impressed markings or striations on the projectiles. This inherent limitation of the system with respect to projectiles has prohibited its use. The biometric imaging and ballistics imaging expertise at Edith Cowan University (ECU) in Australia have developed the next generation of digital imaging and surface profiling information systems for forensic ballistics identification, for solving weapon related crime in Australia and in the international context. The Fireball Firearm Identification System was developed at ECU after the initial research conducted by Smith [1][9] and Cross [1], and later by an ECU software team [12]. The Fireball System was acknowledged as the leading small ballistics identification system in the world [13]. The Fireball has the capability of storing and retrieving images of cartridge case heads, and of interactively obtaining position metrics for the firing-pin impression, ejector mark, and extractor mark. The limitation of this system is that the position and shape of the impression images must be traced manually by the user. For the time being, we still have unsolved problems on projectiles imaging, storing and analyzing although the system has been put in use for nine years already. The efficiency and accuracy of the FireBall system must be improved and increased.

The research papers on the automatic identification of cartridge cases and projectiles are hardly found. L.P. Xin [14] proposed a cartridge case based identification system for firearm authentication. His work was focused on the cartridge cases of center-firing mechanisms.

And he also provided a decision strategy by which the high recognition rate would be achieved interactively. C. Kou et al. [15] described a neural network based model for the identification of chambering marks on cartridge cases. But no experimental results were given in their paper. Using a hierarchical neural network model, a system for identifying the firing pin marks of cartridge cases images automatically is proposed in this paper. We mainly focus on the consideration of rim-firing pin mark identification. A significant contribution towards the efficient and precise identification of cartridge cases in the further processing, such as the locating and coding of ejector marks, extractor marks and chambering marks of cartridge cases will be made through this system. The SOFM neural network and the methods of image processing in our study is described briefly in Section 4. The identification of the ballistics specimen from the crime scene with the test specimen is traditionally conducted by mapping the marks by visual images from a low-powered optical microscope (Fig. 1). The selection of features within the identifying mark is chosen for their apparent uniqueness in an attempt to match both crime scene and test specimens. A decision is made whether the same firearm was responsible for making the marks under examination on the crime scene and test ballistics specimens. The selection of the mark or set of marks for examination and comparison is a critical step in the identification process, and has the capacity to influence subsequent stages in the comparison process [2].



Fig. 1. Landmarks and groove marks of a fired projectile

However, optical and photonic techniques have the capability of a quantum improvement in quality of images for comparison, and as a result will enhance reliability and validity of

the measurements for matching images. The line-scan imaging (Fig. 2) and profilometry techniques [2] [3] each contribute to the information base that will allow identification of firearms from matching crime scene and test fired ballistics specimens.

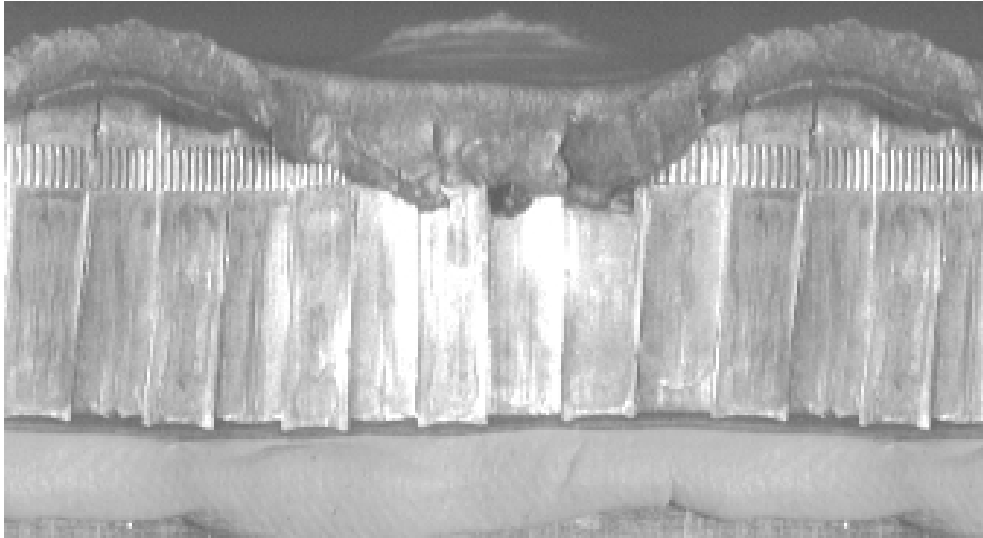


Fig. 2. Linescan image of fired projectile

The development of the line-scan technique [2] [16] [17] for ballistics specimens has the capacity to produce images for the spatial distribution of identification signatures on cylindrical projectiles and cartridge cases. This is achieved by maintaining the surface of the specimen at focus for the rotational scan of the cylinder. However, the production of high resolution images of the cylindrical ballistics specimens are still required for comparison and hence identification.

The difficulties associated with traditional imaging of forensic ballistics specimens are numerous, and include the smallness of the samples, the nature of the surfaces for the cartridge cases (brass) and for the projectiles (lead). As well the features used for identification have low contrast, the cylindrical shape of the cartridge cases, and the distorted shapes of the projectiles (after striking objects) all causing focus problems for image formation.

In this chapter, a new analytic system based on the Fast Fourier Transform (FFT) for identifying the projectile specimens captured by the line-scan imaging technique is proposed. The system gives an approach for projectiles capturing, storing and automatic analysis and makes a significant contribution towards the efficient and precise identification of projectiles. Firstly, in Section 2, the line-scan imaging technique for projectile capturing is described. Secondly, the analytic approach based on FFT for identifying the projectile characteristics and the experimental results are presented in Section 3. The artificial intelligent technologies are applied to the ballistics image classification and identification in Section 4. In Section 5, the image database systems are discussed in details. Some online image processing and visualization applications are covered in Section 6. Finally, suggestions on the further research and conclusion are given in Section 7.

## 2. Line-scan imaging technique for projectile capturing

The proposed analysis system for identifying firearms based on the projectiles images is composed of three parts (shown in Fig. 3), and each part is described in detail in following sections.

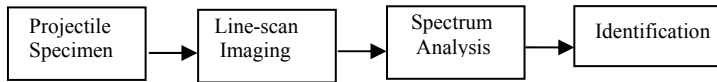


Fig. 3. The proposed analysis system for firearm identification based on projectiles

### 2.1 Line-scan Imaging

Due to the expected high contrast imaging involved in imaging the cylindrical shapes of ballistics specimens, the traditional optical microscopy technique is inherently unsuitable. As the specimen is translated and rotated [17], it is difficult to maintain image quality using oblique lighting on a cylindrical surface at low magnification microscopy. However, in order to obtain the surface information from a cylindrical shaped surface, a line-scan imaging technique is used by scanning consecutive columns of picture information and storing the data in a frame buffer so that a 2D image of the surface of the cylindrical specimen is produced.

The precursor-imaging device to the line-scan camera is the periphery camera, which consists of a slit camera with moving film in order to ‘unwrap’ cylindrical objects by rotating them on a turntable [18]. Relative motion between the line array of sensors in the line-scan camera and the surface being inspected is the feature of the line-scan technique. To achieve this relative motion, the cylindrical ballistics specimen relative to the stationary line array sensors are rotated [17][18][19][20].

Due to the line-scan technique, all points on the imaging line of the sample are in focus. This is because the cylindrical ballistics specimen is rotated about an axis of rotation relative to a stationary line array of sensor. Thus, during one full rotation of the cylindrical ballistics specimen, all points on the rotating surface will be captured on the collated image. [17].

The line-scan imaging analysis system for projectiles in our study is shown in Fig. 4. The stepper motor rotates with 360 degrees/ 2400 steps, namely 0.15 degree each step. The 0.15 degree stepper motor is used in order to acquire sufficient details from the surface of the projectile. For example, a projectile with a diameter of 5-15mm has a perimeter range of 15-50mm roughly. With 2400 steps a round the lowest resolution of the line-scan image will still be  $2400/50=48$  lines per mm. A CCD camera (Sony, Model DXC-151AP) is used instead of the traditional camera used in [17] [18]. The graphic capturing card installed in the PC has an image size of  $320 \times 240$  pixels. A ring light source (Leica 30120202) is adopted, which can provide uniform lighting conditions [21]. The optical system used was just a standard optical microscope (Leica MZ6).

Being quite different from the method used in [17] [18], the procedure in our line-scan imaging approach is as follows:

1. With the stepper motor's every step
2. the CCD camera captures the current image of projectile specimen and
3. sends the image to Graphic card in PC;
4. The middle column of pixels in this image is extracted and saved consecutively in an array in the buffer on PC, and

5. steps 1. and 2. are repeated until the whole surface of the projectile specimen is scanned;
6. The array in the buffer is used to produce a 2-D line-scanned image for the whole surface of the projectile.

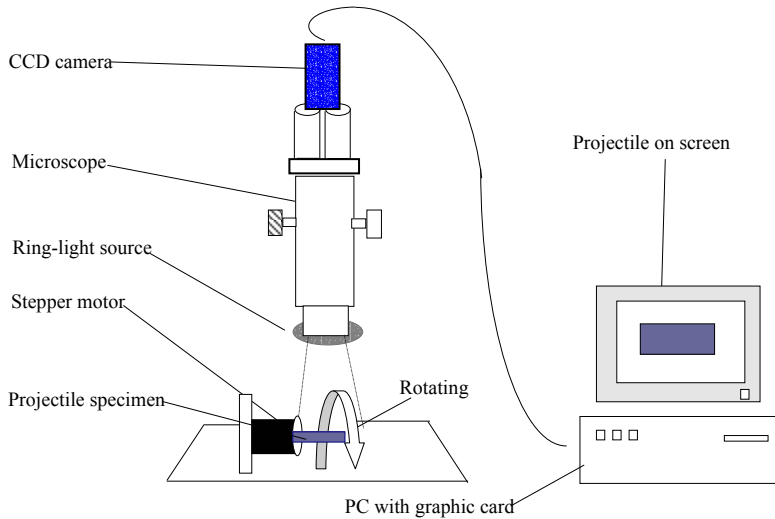


Fig. 4. The line-scan imaging and analyzing system

The resolution of the line-scan image is dependent on,

- the rotational degree per step of the stepper motor
- the resolution of CCD camera
- the resolution of graphic capturing card
- the columns captured at each step in step

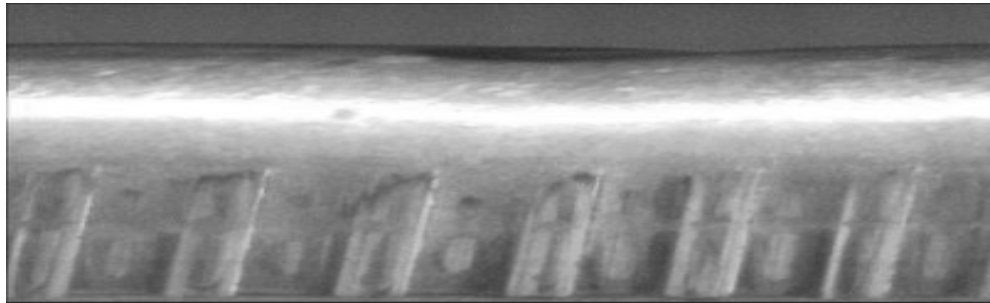
By adjusting the length of each step of the stepper motor and the number of columns captured in each step to meet forensic investigation requirements, the resolution of the line-scanned image of projectile specimen could be manipulated. The resolution required to detect the major striations on land marks and groove marks is not necessary to be very high. The line-scan image resolution is set by the rotational steps and sizes of the projectile specimen.

## 2.2 Projectile specimens and their line-scanned images

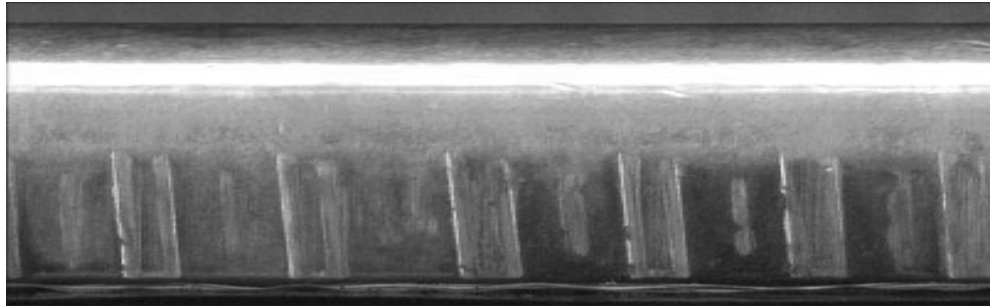
The projectile specimens in our study, provided by Western Australia Police Department, are in four classes and belong to four different guns. They are:

1. Browning, semiautomatic pistol, caliber 9mm.
2. Norinco, semiautomatic pistol, caliber 9mm.
3. and 4. Long Rifle, semiautomatic pistol, caliber 22 (5.59mm).

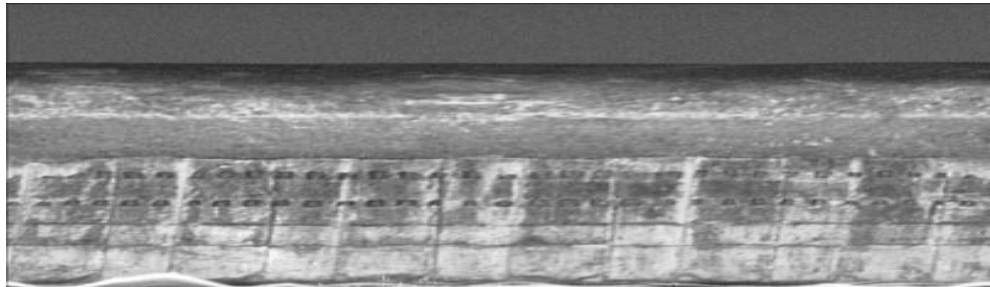
Through the use of the line scan imaging technique as discussed in Section 2.1, all the projectile specimens in our study are recorded under the same conditions (e.g light conditions, the stepping angle of the stepper motor etc...). All the landmarks and groove marks of projectile specimen are captured and displayed in the line scanned image through adjusting the stepping angle of the stepper motor by just one full rotation (360 degrees).



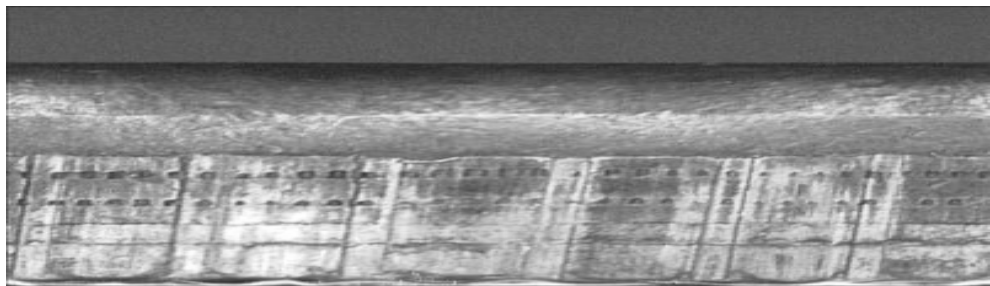
a



b



c



d

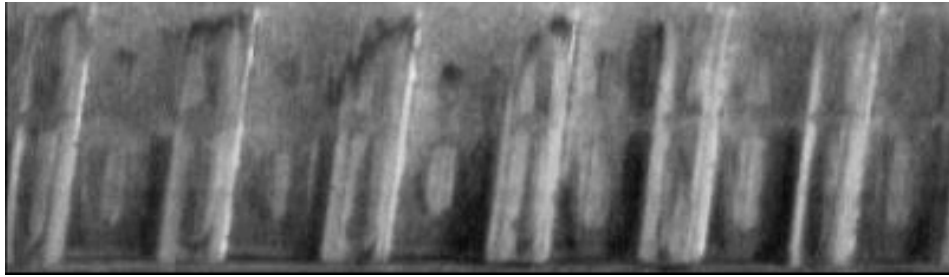
Fig. 5. Four classes of line-scanned images of projectiles in our study (with code: a, 101; b, 201; c, 301; d, 401)

Line-scanned images of four classes of projectile specimens in our study are shown Fig. 5. For the purpose of firearm identification, what we are looking at in these images are some unique features such as land mark width, groove mark width, and their orientations. Obviously there are many more different features (visible or hidden) in the different images. All those features form a unique combination for each every weapon as a set of fingerprints for that particular weapon.

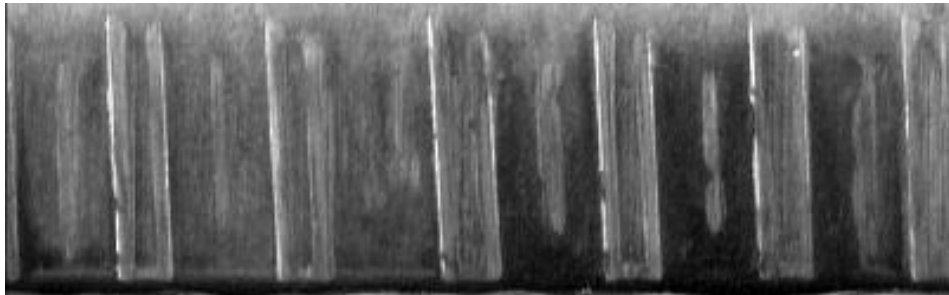
### 2.3 Image pre-processing for FFT analysis

In a practical application, the quality of the line-scanned image of a projectile specimen can be affected and noised by many factors such as the lighting conditions, the materials of the specimen, the original texture on the surface of specimen, and the deformed shapes. Strong noise and damage in the line-scanned image may result, and this would mean difficulties in extracting and verifying the important features used for identifying the individual specimen, such as the contours, edges, the directions and the width (or distance) of land marks and groove marks. To eradicate or minimize the effects mentioned above, the following image pre-processing operations are applied to the line-scanned images obtained in Section 2.2.

A general function of image preprocessing is the contrast enhancement transformation [22]. Low-contrast images can be a result of poor lighting conditions, lack of dynamic range of the imaging sensor, and a wrong setting of lens aperture during image acquisition. Increasing the dynamic range of gray levels in the image being processed is the idea behind contrast enhancement. In our study, the images are often blurred to a certain extent due to the reason of the strong reflection from the metal surface. The landmarks or groove marks may be hidden within. Thus, the contrast enhancement transformation is used upon the images obtained in Section 2.2. We perform a simple contrast enhancement by linearly expanding the contrast range by assigning the darkest pixel value to black, the brightest value to white, and each of others to linearly interpolated shades of grey in the image. The operation is automated when acquiring the images with a CCD camera. In the line-scanned images, only the regions that include the landmarks and groove marks are useful for analyzing and identifying the characteristics of the projectile specimens. Thus, we only select the regions in images that are necessary and useful to our study. The images (the effective regions in original images) shown in Fig. 6 are transformed versions corresponding to the images in Fig. 5 by the region selecting and the contrast enhancement transformation. One of the most important roles in the identification system is feature extraction. There are many ways to perform edge detection. However, the most may be grouped into two categories, Gradient and Laplacian. The gradient method detects the edges by looking for the maximum and minimum in the first derivative of the image. The Laplacian method searches for zero-crossings in the second derivative of the image to find edges. For detection of edge and lines in our line-scan images of projectiles, various detection operators can be used. Most of these are applied with convolution masks and most of these are based on differential operations. We pick up the first derivatives [22] as the images features. For a digital image, Sobel operators in vertical and horizontal directions (shown in Fig. 7 with  $3 \times 3$  window) are the most popular powerful masks used to approximate the gradient of  $f$  at coordinate  $(i, j)$ . In our experiments, we adopt the Sobel operators to extract the contours and edges of the land and groove marks on line-scanned images of projectile specimens, which convolves the images with the Sobel masks to produce the edge maps of the four line-scan images shown in Fig. 8. Because the directions of the land and the groove marks of the projectile specimens are mostly along 90 degrees in the line-scanned images,



a



b



c

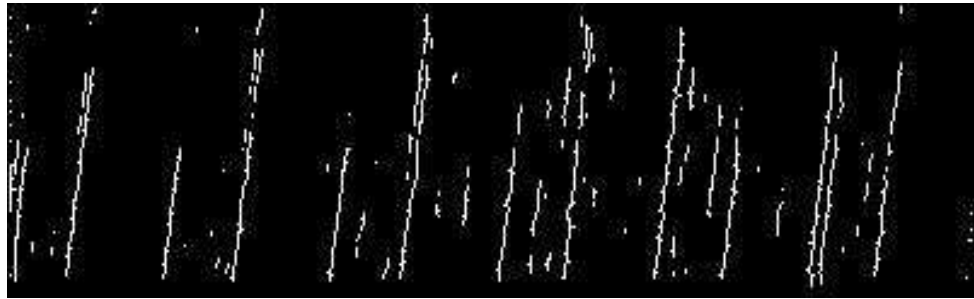


d

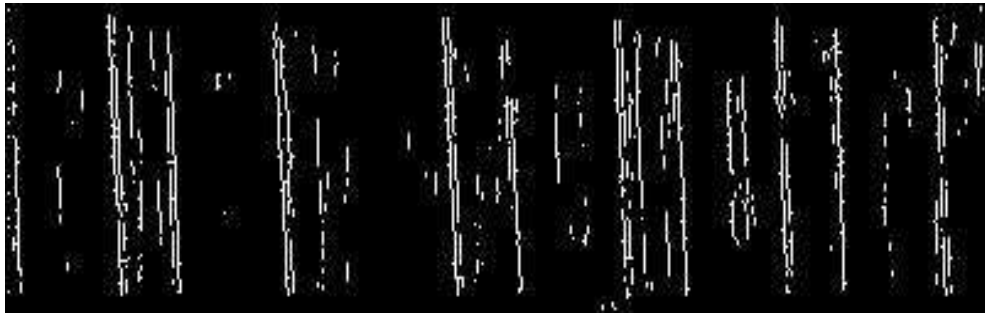
Fig. 6. Contrast enhancement results (a, b with size  $400 \times 110$ , and c, d with size  $400 \times 100$ )

-1	-2	-1	-1	0	1
0	0	0	-2	0	2
1	2	3	-1	0	3

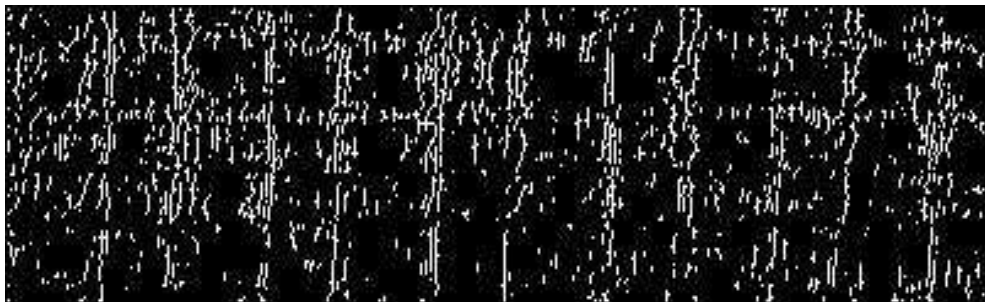
Fig. 7. Sobel masks in vertical and horizontal directions



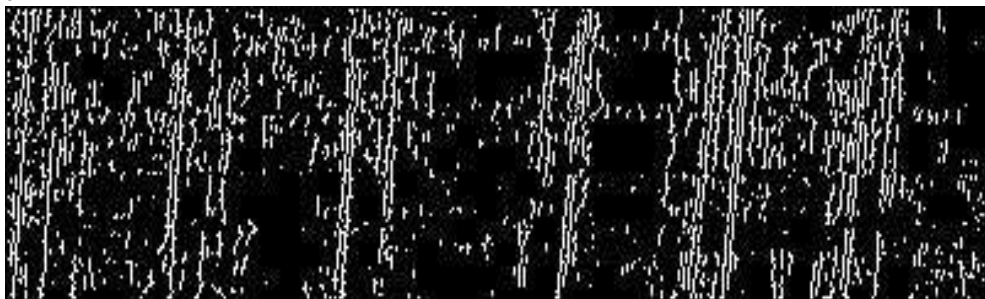
a



b



c



d

Fig. 8. The contours and edges extracting using Sobel operator in vertical direction

we only adopt the vertical direction mask (Fig. 7) for extracting the features of the line-scanned images. Through an observation of Fig. 8 in which there are lots of noises and disconnection on the land and groove marks, the conventional spatial techniques are not suitable for the nature of locally. Hence, a FFT-based analysis for projectiles is introduced.

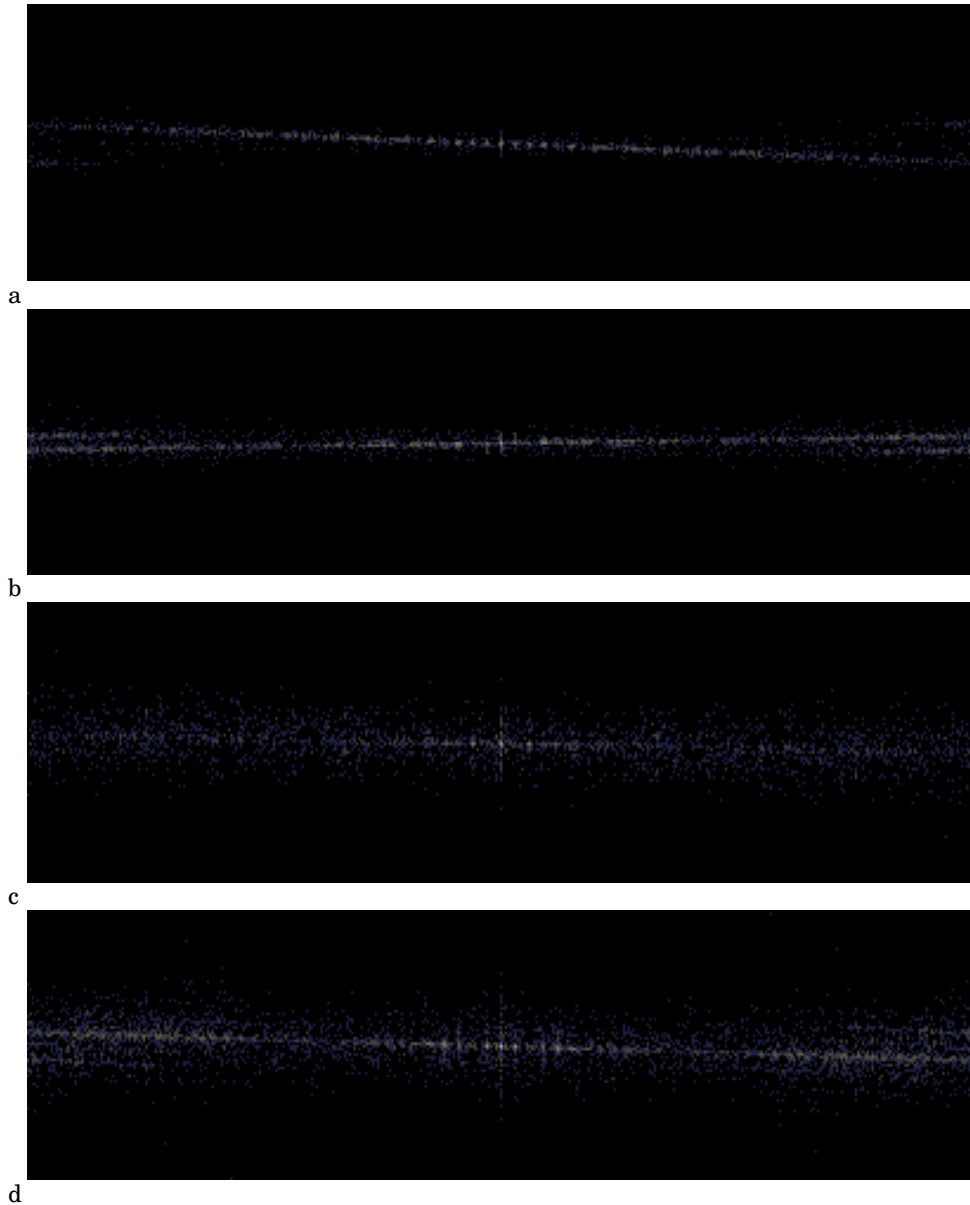


Fig. 9. Fourier transformation results of the images in Fig. 8

### 3. FFT-based analysis

#### 3.1 FFT and spectrum analysis

The Fourier transform of a two-dimensional, discrete function (image),  $f(x, y)$ , of size  $M \times N$ , is given by the equation

$$F(u, v) = \frac{1}{MN} \sum_{x=0}^{M-1} \sum_{y=0}^{N-1} f(x, y) e^{-j2\pi(ux/M + vy/N)} \quad (1)$$

where  $j = \sqrt{-1}$ , for all  $u = 0, 1, 2, \dots, M-1, v = 0, 1, 2, \dots, N-1$ . We define the Fourier spectrum by the equation

$$|F(u, v)| = [R^2(u, v) + I^2(u, v)]^{1/2} \quad (2)$$

where  $R(u, v)$  and  $I(u, v)$  are the real and imaginary parts of  $F(u, v)$ , respectively.

For describing the directionality of periodic or almost periodic 2-D patterns in an image, the Fourier spectrum is ideal. As easily distinguishable as concentrations of high-energy burst in the spectrum, these global texture patterns are generally not convenient to detect with spatial methods because of the local nature of these techniques. In the feature extraction process some of texture descriptors are considered both in Fourier and spatial domains. It is noticed that some of spatial domain descriptors can be used with success for geology recordings where the image appears to be very similar to the one in this research [23].

For the specific research interests in this study we only consider a set of features of the Fourier spectrum that are used for analyzing and describing the line-scanned images of projectiles:

1. Principal direction of the texture patterns are shown by prominent peaks in the spectrum.
2. Fundamental spatial period of the patterns are shown by the location of the peaks in the frequency plane.
3. Some statistical features of the spectrum.

By expressing the spectrum in polar coordinates to yield a function  $S(r, \theta)$ , where  $S$  is the spectrum function, and  $r$  and  $\theta$  are the variables in this coordinate system, detection and interpretation of the spectrum features just mentioned often are simplified. For each direction  $\theta$ ,  $S(r, \theta)$  is a 1-D function  $S_\theta(r)$ . Similarly, for each frequency  $r$ ,  $S_r(\theta)$  is a 1-D function. Analyzing  $S_\theta(r)$  for a fixed value of  $\theta$  yields the behavior of the spectrum (such as the presence of peaks) along a radial direction from the origin, whereas analyzing  $S_r(\theta)$  for a fixed value of  $r$  yields the behavior along a circle centered on the origin. A more global description is obtained by integrating (summing for discrete variables) these functions [22]:

$$S(r) = \sum_{\theta=0}^{\pi} S_\theta(r) \quad (3)$$

and

$$S(\theta) = \sum_{r=1}^{R_0} S_r(\theta) \quad (4)$$

where  $R_0$  is the radius of a circle centered at origin.

The results of Equations (3) and (4) constitute a pair of values  $[S(r), S(\theta)]$  for each pair of coordinates  $(r, \theta)$ . We can generate two 1-D functions,  $S(r)$  and  $S(\theta)$ , that constitute a spectral-energy description of texture for an entire image or region under consideration by varying these coordinates. Furthermore, descriptors of these functions themselves can be computed in order to characterize their behavior quantitatively, which can be used as ballistics features for firearm identification.

### 3.2 FFT-based analysis, identification and experimental results

The following section discusses in detail some characteristics and descriptors of the line-scanned images for identification of projectiles using the radius spectrum and angular spectrum.

We know that the slowest varying frequency component ( $u = v = 0$ ) corresponds to the average gray level of an image. The low frequencies correspond to the slowly varying components of an image as we move away from the origin of the transform. In a line-scanned image of projectile specimen, for example, these might correspond to the land and groove marks which are large in scale and regular in shape. Moving further away from the starting point, the higher frequencies begin to correspond to faster and faster gray level changes in the image. These are the small or irregular marks and other components of an image characterized by abrupt changes in gray level, such as noises. Now we focus our attention on the analysis of low frequencies in the radius and angle spectrum of line-scanned images.

Shown in Fig. 10 a, b, c and d, are the plots of radius and angle spectrum corresponding to images in Fig. 9 a, b respectively. The results of FFT clearly exhibit directional 'energy' distributions of the surface texture between class one and two. Comparing Fig. 10 a to b, the plots on the radius spectrum, six clear peaks in the range of low frequencies ( $r < 20$ ) can be observed on the former whilst the latter has only three peaks in the same range and is smooth in shape, this indicates that 'energy' of the class one specimen is distributed in several permanent positions, and also reveals that the class one specimen has a coarse surface texture and the wide land and groove marks, while the surface texture of class two is fine and the smaller widths of land and groove marks.

The angular spectrums (Fig. 10 c and d) display a great distinctness in position of prominent peaks between class one and two. With respect to the measurement coordinate, further study reveals that the angular spectrum can clearly indicate the angular position of periodic grooves or scratches on the surface. It can be seen from the angular spectrum there is a maximum peak at about 81 degrees in Fig. 10 c. This is indicative of scratches (the land or groove marks) oriented 81 degrees to the surface of the projectiles, while the maximum peak in Fig. 10 d sits at about 95 degree. Furthermore, a second prominent peak of about 100 degrees (corresponding to small or shallow marks on the projectile's surface) can be seen on the former plot. However, it is noted that the second peak of Fig. 10 d is at about 85 degree.

By examining quantitative differences of spectrums using a set of features, the characteristics of projectile specimen surface textures can also be revealed.

To compare and analyze the spectrum differences between the two classes easily, a set of features is used, and the quantitative results are shown in Table 1 (where,  $r_1$  and  $a_2$ , Max;  $r_2$  and  $a_3$ , Mean;  $r_3$  and  $a_4$ , Std;  $r_4$  and  $a_5$ , Max; Median; and  $a_1$ , Position of maximum peak).

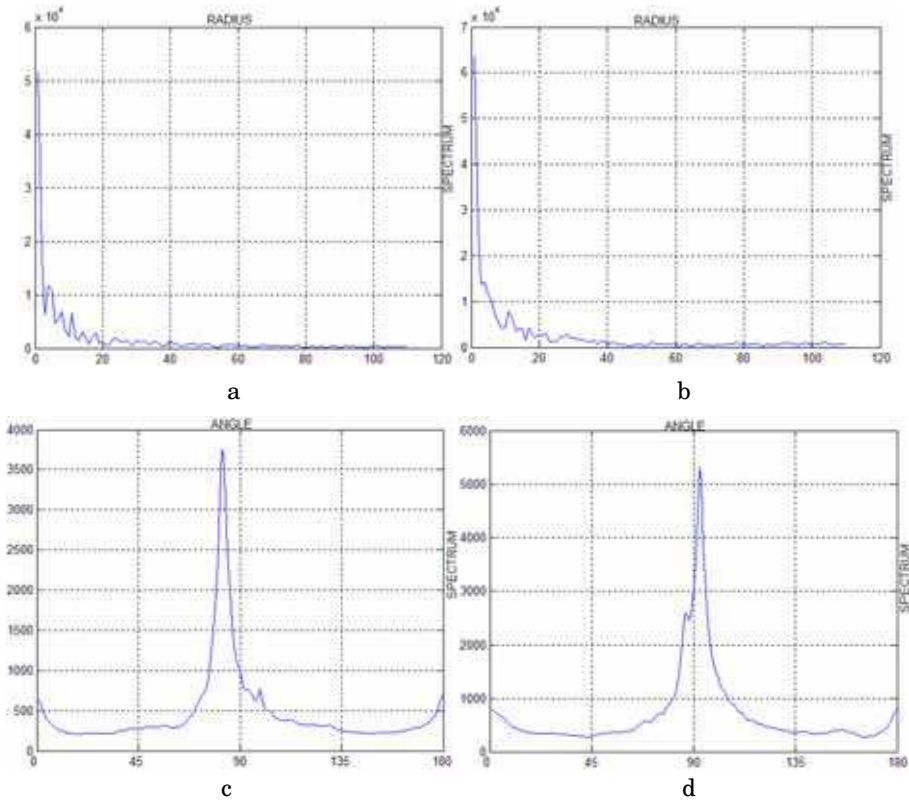


Fig. 10. Radial spectrum (a, b) and Angular spectrum (c, d) of the images (a, b) in Fig. 9

As observed from Table 1, the Max, Mean, and Std of class one are relatively smaller than class two, while the relative variation for radio between Max and Mean is greater. The difference between prominent peaks (corresponding to the orientations of land and groove marks) of class one and two is 14 degrees. All this goes to show that FFT spectrum analysis, in the form of quantification, can reveal characteristic and directional surface textures of the projectile specimen.

Class	Code	Radial spectrum				Angular spectrum				
		$r_1$	$r_2$	$r_3$	$r_4$	$\alpha_1$	$\alpha_2$	$\alpha_3$	$\alpha_4$	$\alpha_5$
1	101	51517	1728	5372	29.81	81	3753	475.2	546.2	7.898
2	201	63646	2538	6809	25.07	95	5308	697.9	794.7	7.600

Table 1. Radial spectrum and angular spectrum statistics results of Fig. 9 a and b

After obtaining the initial significant results, the 12 more experiments involving 12 new projectile specimens fired by 12 different weapons are carried out. Those 12 specimens are among the four classes of weapons discussed in the section 2.2 and coded in Fig. 5 (4 in class 1, code 102-105; 2 in class 2, code 202-203; 3 in class 3, code 302-304; and 3 in class 4, code 402-404). Table 2 lists all the experimental results based on the total 16 projectile specimens in our study.

Class	Code	Radial spectrum				Angular spectrum				
		$r_1$	$r_2$	$r_3$	$r_4$	$a_1$	$a_2$	$a_3$	$a_4$	$a_5$
1	101	51517	1728	5372	29.81	81	3753	475.2	546.2	7.898
	102	51162	1591	5187	32.16	81	3709	437.6	545.6	8.487
	103	51200	1520	5087	33.68	81	3583	418.2	509.8	8.571
	104	51556	1699	5348	30.34	81	3589	467.3	514.1	7.685
	105	62715	1962	6299	31.96	81	4219	539.5	617.8	7.827
2	201	63646	2538	6809	25.07	95	5308	697.9	794.7	7.600
	202	64381	2738	7038	23.51	95	5257	752.9	777.7	6.990
	203	64059	2545	6707	25.16	95	5193	700.0	794.0	7.419
3	301	63959	2899	6942	22.06	86	2514	724.7	451.9	3.469
	302	64448	2478	6889	26.01	86	2714	719.4	445.5	3.774
	303	64288	2743	7090	23.43	86	2517	685.8	439.9	3.669
	304	63694	3011	6999	21.23	86	2750	752.7	512.8	3.657
4	401	76059	4040	8554	18.27	79	4965	1010	787.8	4.916
	402	76406	5026	8982	15.20	79	4972	1256	835.6	3.959
	403	75607	3735	8035	20.23	79	4897	933.9	753.3	5.249
	404	76796	3786	8498	20.28	79	4135	946.3	738.6	4.371

Table 2. Radial spectrum and angular spectrum statistics results based on the specimens in our study

By observing Table 2 and recalling that the calibers of class one and two are the same, and so are the class three and fours, we can easily identify the projectiles into a class using the features listed in Table 2. For example, all the values of  $r_4$  for class one are greater than 28.0, while for class two, none is greater than 26.0. In order to identify the firearms to the level of the single gun we treat each every row of the table 2 as a set of fingerprints from that gun. The characteristics ( $r_1$ - $r_4$  and  $a_1$ -  $a_5$ ) we used in spectrum analysis can be formed as a set of features vectors for building an artificial intelligent (AI) system for the automatic firearm identification based on the spent projectiles. Several AI algorithms are under investigation to best use the spectrum characteristics as searching criteria in the existing FireBall firearm identification database.

#### 4. SOFM and cartridge case image processing

It is hard to find research papers on the automatic identification of cartridge. A cartridge cases based identification system for firearm authentication was proposed by Le-Ping Xin [14]. His work was focused on the cartridge cases of center-fire mechanism. And he also provided a decision strategy from which the high recognition rate would be achieved interactively. A neural network based model for the identification of the chambering marks on cartridge cases was described by Chenyuan Kou et al. [24]. But no experiment results were given in their paper.

In this section a proposed hierarchical firearm identification model based on cartridge cases images is shown. The following parts, describe respectively, the structure of the model, the training, testing of SOFM, and decision-making strategy.

#### 4.1 SOFM neural network

The basic classifying units in our identification system is picked as the Self-Organizing Feature Map (SOFM) neural networks. The SOFM has been applied to the study of complex problems such as speech recognition, combinatorial optimization, control, pattern recognition and modeling of the structure of the visual cortex [25], [26], [27] and [28]. The SOFM we used is a kind of un-supervised neural network models, it in effect depicts the result of a vector quantization algorithm that places a number of reference or codebook vectors into a high-dimension input data space to approximate defined values between the reference vectors, the relative values of the latter are made to depend on it to its data set in an ordered fashion. When local-order relations are each other as if there neighboring values would lies along an “elastic surface”. This “surface” becomes defined as a kind of nonlinear regression of the reference vectors through the data points [29], by means of the self-organizing algorithm.

We employ the standard Kohonen’s SOFM algorithm summarized in Table 3, the topology of SOFM is shown in Fig. 11.

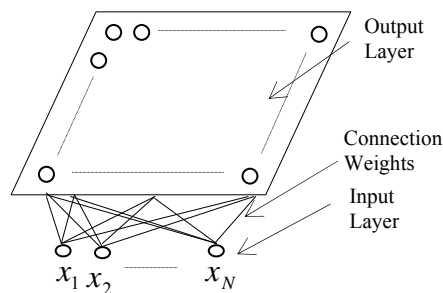


Fig. 11. The topology of SOFM

##### 4.1.1 Identification model

The system proposed comprises of three stages as shown in Fig. 12, the preprocessing stage as mentioned in Section 2 and Section 3, the classification stage based on neural networks involving two levels SOFM neural networks and the decision-making stage. In our study, the two levels SOFM neural networks are:

The first level has one SOFM neural network (as shown in Fig. 11) labeled by  $\text{SOFM}_0$  which acts as a coarse classifier among the training (or testing) patterns presented to it. The training or learning processing is the same as that mentioned in Section 4.1.2, which belongs to the unsupervised learning type.

Comprising several child SOFM networks denoted by  $\text{SOFM}_i$   $i = 1, 2, \dots, n$ , where  $n$  is the number of child SOFM networks is the second level of neural networks, making fine identification among the patterns classified by  $\text{SOFM}_0$  (or the output of  $\text{SOFM}_0$ ).

##### 4.1.2 Training

In our study, The training or learning processing for  $\text{SOFM}_0$  is identical to that mentioned in Table 3, which belongs to the type of unsupervised learning (we use the images of  $C$  to train the  $\text{SOFM}_0$ . The number of neurons in input layer is  $48 \times 196$ , corresponding to the size of

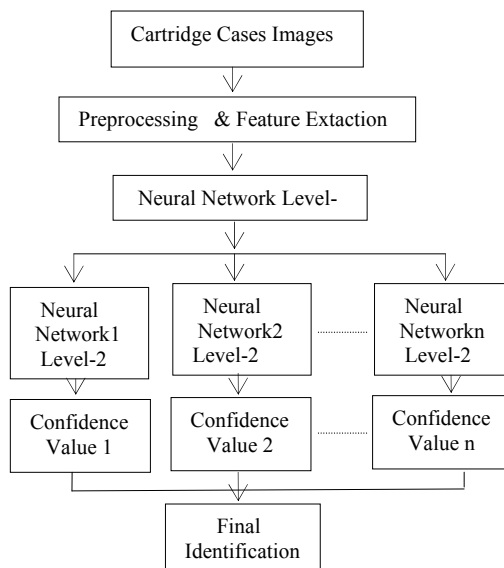


Fig. 12. The proposed identification system

windows normalized (as mentioned before). In the training phase, when a neuron of output layer is inactive for a period of time, it is removed from the network. If a neuron is not chosen frequently as the winner over a finite time interval, it may be considered inactive. After being trained, the neurons, which are active with high output value in the output layer of  $SOFM_0$ , stand for the classes to which the training images (or the testing specimens) belong. Due to the result of classification of  $SOFM_0$  in our study, the training set  $C$  has been parted into several subsets. Combination of these subsets in a proper manner achieve training sets for the  $SOFMs$  at the second level. When the positions of two classes in the output layer are very close or overlapping the second level  $SOFM$  neural networks are generated. The training sets are formed by combining the twoclass patterns for those that are close or overlapping. This training process is identical to that of  $SOFM_0$ .

#### 4.1.3 Testing

The testing procedure for firearm identification system is as follows:

- Step 1. Using a selected testing cartridge case image from the testing set  $T$ , present this testing pattern to the first stage of the identification system--the preprocessing stage.
- Step 2. Select a type of window from all types in turn, and move this window over the testing pattern processed in Step1 at every location by every pixel horizontally and vertically, pick up the sub-images.
- Step 3. Using Formula (5) calculated the confidence values for each sub-image, to do this, present all the sub-images to the  $SOFM_0$  in turn, and then to  $SOFM_i$ ; by the result of  $SOFM_0$ . Return Step2 until all type windows are used up.
- Step 4. These confident values are presented to the third stage which is the decision making stage, and using Formula (6) and (7), the final result for the testing cartridge case image is calculated.

## Thank You for previewing this eBook

You can read the full version of this eBook in different formats:

- HTML (Free /Available to everyone)
- PDF / TXT (Available to V.I.P. members. Free Standard members can access up to 5 PDF/TXT eBooks per month each month)
- Epub & Mobipocket (Exclusive to V.I.P. members)

To download this full book, simply select the format you desire below

